J. Physiol. (1983), **343**, *pp.* 85–104
With 3 plates and 4 text-figures
Printed in Great Britain

THE NUMBER OF SYNAPTIC BOUTONS TERMINATING ON *XENOPUS* CARDIAC GANGLION CELLS IS DIRECTLY CORRELATED WITH CELL SIZE

BY PETER B. SARGENT

From the Department of Structural Biology, Sherman Fairchild Building, Stanford University School of Medicine, Stanford, CA 94305, U.S.A.

(*Received 17 September 1982*)

SUMMARY

1. The relationship between the size of parasympathetic neurones and the number of synaptic boutons terminating upon them has been studied in the cardiac ganglion of *Xenopus laevis*. Synaptic boutons were visualized by impregnation with zinc iodide and osmium (ZIO), which by electron microscopy was shown to stain heavily all synaptic boutons in six preparations.

2. Light microscopic examination of the unipolar ganglion cells in intact tissue reveals that larger neurones have more synaptic boutons. The number of boutons terminating on the cell body is significantly correlated with its surface area. By statistical means it was possible to demonstrate that the relation between bouton number and surface area is linear and that the regression line has a y-intercept not significantly different from zero. Therefore the density of synaptic boutons, one per 127 μm^2 of cell body surface, is independent of cell size.

3. The size of synaptic boutons, measured as the area of apposition between bouton and cell body, is similar for small and for large ganglion cells; thus a constant fraction (2 %) of the cell body on average is covered by synaptic boutons, regardless of cell size.

4. The correlation between bouton number and cell body surface area is not the result of interaction between boutons. The frequency distribution of boutons per normalized cell was found to be similar to that expected from the Poisson distribution. Thus the probability that a bouton will be 'assigned' to a particular cell is independent of how many other boutons are present. The only factor that appears to influence the number of boutons on the cell body is its size.

INTRODUCTION

In both amphibian and mammalian skeletal muscle the size of motor nerve terminals is correlated with myofibre diameter: larger fibres are supplied by larger terminals (Harris, 1954; Coërs, 1955; Nyström, 1968; Kuno, Turkanis & Weakly, 1971; Korneliussen & Waerhung, 1973; Harris & Ribchester, 1979). Since nerve terminal size is positively correlated with transmitter release (Kuno *et al.* 1971; Bennett & Raftos, 1977; Harris & Ribchester, 1979, Grinnell & Herrera, 1980), there

will be more transmitter release generally from terminals on larger fibres. The incremental release onto larger fibres tends to compensate for their decreased input resistance and may tend to 'normalize' the safety factor for transmission on fibres of varying sizes (Kuno *et al.* 1971; see also Nudell & Grinnell, 1982).

Here anatomical techniques are used to document a direct correlation between the size of autonomic neurones in the *Xenopus* cardiac ganglion and the number of synaptic boutons made upon them. The observed relationship has the form expected of a scheme designed to assure a constant safety factor for transmission on neurones of varying sizes. Preliminary accounts of this work have been published (Sargent & Evans, 1981; Sargent, 1982).

METHODS

Xenopus laevis (4·4–6·5 cm body length) were obtained from Nasco, Inc., Fort Atkinson, WI, and were killed by decapitation and pithing. Interatrial septa were dissected in frog Ringer solution and pinned to the bottom of Petri dishes containing Sylgard 184 (Dow Chemical Co., Midland, MI). The composition of frog Ringer solution was (in mM): NaCl, 114; KCl, 2; $CaCl_2$, 1·8; HEPES, 2; pH 7·4.

Zinc iodide–osmium staining

Interatrial septa were immersed for 1 hr at room temperature (20–23 °C) in a solution containing 4 ml. zinc iodide (9 g Zn, 4·5 g I_2, 120 ml. H_2O), 4 ml. 0·36 M-potassium acetate, pH 4·5, and 0·6 ml. 4% OsO_4.

For light microscopic examination septa were rinsed briefly in several changes of frog Ringer solution, dehydrated in ethanol, cleared in xylene and mounted between a pair of large cover-slips. For electron microscopic examination septa were rinsed in Ringer solution, post-fixed for 1 hr with 1% glutaraldehyde in 61 mM-sodium phosphate, pH 7·2, rinsed in Ringer solution, dehydrated in ethanol and embedded in thin wafers of Epon–araldite. Regions of septa containing nerve trunks were removed from the wafers and polymerized to blank Beem capsules using Epon–araldite. Thin sections having silver interference colour were cut on an AO Ultracut ultramicrotome and grid-stained with methanolic uranyl acetate and with lead citrate (Heuser & Reese, 1973).

Quantitative staining of synaptic boutons

The optimum conditions for staining cardiac ganglia with zinc iodide and osmium (ZIO) (Maillet, 1962) were determined in a set of preliminary experiments in which several staining parameters were systematically altered, notably pH, time, osmium concentration, and buffer concentration. Not all changes affected nerve terminal and 'non-specific' staining equally, and it was possible to identify a set of conditions that reliably and heavily stained synaptic boutons and that stained very few other structures (Pl. 1). The measured osmolarity of the optimum staining solution, 550 m-osM, is considerably higher than frog Ringer solution, owing to the high concentration of potassium acetate. The use of lower buffer concentration (0·036 M in place of 0·36 M) permitted the staining to proceed under roughly iso-osmotic conditions (280 m-osM) but was accompanied by more 'non-specific' staining, especially of the Golgi complex, and by the appearance of a precipitate on the surface of the septum (data not shown). The hyperosmotic formulation is clearly superior for an analysis of synaptic boutons in intact interatrial septa. In the following paragraphs evidence is presented that this formulation consistently stains all synaptic boutons and that it does not result in tissue shrinkage as compared with the more iso-osmotic formulation.

Iso-osmotic staining. An electron microscopic analysis of ganglion cells stained with the 280 m-osM-ZIO solution revealed the presence of dense reaction product within synaptic terminals and within membrane-bound organelles in the ganglion cell body (Pl. 2*A*); these structures appear to be lysosomes and correspond to the small, stained organelles seen within the cytoplasm by light microscopy (Pl. 1; see also McMahan & Kuffler, 1971). Although the reaction product was found throughout the synaptic terminal, dense deposits of stain corresponding in size and shape to synaptic vesicles were evident (Pl. 2*B*, arrows). When interatrial septa were stained for 20 min rather than 1 hr, reaction product was found only within small vesicles (data not shown). Large,

dense-cored vesicles are not impregnated with stain (Pl. 2*B*, arrowhead; see also Akert & Sandri, 1968).

The consistency with which synaptic terminals were stained with the 280 m-osM-ZIO solution was assessed by electron microscopy after staining two interatrial septa on each of three days. Boutons were located by scanning ganglion cell perimeters at a final magnification of 66,000 ×; vesicle-containing profiles on the ganglion cell surface were judged to be synaptic boutons when situated opposite punctate electron densities in the ganglion cell membrane (Pl. 2*B*). Boutons were scored as being heavily labelled (as in Pl. 2*B*), lightly labelled (with reaction product present in some of the small synaptic vesicles and sparsely in the extravesicular cytosol), or unlabelled. All 141 boutons in six preparations were labelled by the staining procedure; 91 % of the boutons were heavily labelled, and the remaining boutons were lightly labelled. The staining protocol thus consistently impregnates all synaptic boutons in all preparations; at least 90 % of the boutons, on average, were heavily stained and would be visible presumably in intact septa using light microscopy.

Hyperosmotic staining. Ganglion cells treated with the hyperosmotic (550 m-osM)-ZIO solution and examined in the electron microscope again were seen to have stained nerve terminals on their surface and stained lysosomes within their cytoplasm (Pl. 3*A*). Increasing the buffer concentration to produce hyperosmotic conditions improves the usefulness of the stain in two ways: first, as seen in the light microscope nerve terminals are generally more darkly stained with the hyperosmotic formulation than with the iso-osmotic one. This observation was confirmed by electron microscopy: all 150 synapses examined in a total of six preparations treated with the hyperosmotic formulation were heavily labelled with reaction product (Pl. 3*B*). A second consequence of using the hyperosmotic formulation was that reaction product was associated less often with structures other than nerve terminals (e.g. extracellular matrix, compare Pl. 2*A* with Pl. 3*A*). However, an additional effect of using the hyperosmotic ZIO mixture is that ganglion cells are crenulated (Pl. 3*A*) possibly owing to the loss of water from the ganglion cell and its accumulation beneath the satellite cell. In order to assess the extent to which shrinkage may affect the measurements, two interatrial septa were stained with each ZIO solution (hyperosmotic and 'iso-osmotic'), and the following parameters were measured and compared: ganglion cell body size, bouton size, and bouton number per cell body. The mean values for each parameter were comparable or identical for septa stained with each of the formulations (cell body size: 25 ± 6 (long axis) $\times 19 \pm 5$ μm (short axis) for 280 m-osM data, $25 \pm 6 \times 18 \pm 5$ μm for 550 m-osM data; bouton size: $2{\cdot}7 \pm 1{\cdot}8$ μm^2 for 280 m-osM data, $2{\cdot}9 \pm 1{\cdot}9$ μm^2 for 550 m-osM data; bouton number per cell body: 11 ± 6 for 280 m-osM data, 11 ± 6 for 550 m-osM data; all values are mean $\pm$ S.D., $n \geqslant 100$ cells). Thus the 550 m-osM formulation stains all synapses heavily, and it neither produces measurable shrinkage in cell or bouton size nor alters the number of counted boutons per cell body as compared with the 280 m-osM formulation. Despite its unphysiological osmolarity, the 550 m-osM formulation appears to produce an accurate picture both of the size of ganglion cells and of the number of synaptic boutons per cell body. Bouton staining with 550 m-osM-ZIO solution is therefore suitable for analysing the relationship between cell size and bouton number in adult *Xenopus* cardiac ganglia. It should be noted that the ZIO formulation used here is *not* likely to be useful in other preparations without modification; for example, it does not produce satisfactory staining of synaptic boutons in cardiac ganglia of *Xenopus* larvae unless both the pH and the time of staining are increased.

Comparing the number of synaptic boutons with cell body size

The relationship between cell body size and bouton number was measured for thirty to seventy cells in each of eleven interatrial septa. Although each septum contains several hundred neurones, only a fraction of these are situated so as to permit an unambiguous determination of their pattern of innervation. Neurones whose cell bodies were closely applied to the nerve trunks were not analysed, as the trunks contain many densely stained axons. Likewise, measurements were not made from neurones lying in small neuronal clusters (e.g. as in fig. 3*a* of McMahan & Kuffler, 1971), since boutons situated between two closely apposed neuronal cell bodies could not be unambiguously assigned to a particular ganglion cell. To avoid biasing the data a nerve trunk containing many ganglion cells was chosen at low magnification (100 ×), and measurements were taken from each isolated neurone (at 1000 ×) encountered along the trunk until at least thirty ganglion cells had been so analysed (mean number of cells analysed per septum: forty-six).

Two procedures were used for recording bouton number and cell size. The two procedures

produced similar results when used to make measurements on common septa (data not shown). On four septa (Nos. 1–4 in Table 1) the axes of the ganglion cell body were measured with an eyepiece micrometer, and the boutons were counted by focusing through the cell. On seven other septa a drawing of the outline of the cell at the focal plane of its greatest cross-sectional area was drawn using a Zeiss camera lucida attachment, and the centre of each bouton was indicated (without regard to its position on the 'top' or 'bottom' half of the cell). Measurements were then made from the drawings. As described below this second technique permitted a crude analysis of the spatial distribution of boutons on the cell surface.

The shape of ganglion cells. Ganglion cells of interatrial septa viewed *en face* often have a roughly elliptical shape (Pl. 2*A*; the plane of this thin section is identical to the plane of focus of cells viewed by light microscopy). The shape of these cell bodies is approximated by prolate ellipsoids having their major axis in the focal plane, since (1) as one focuses through a ganglion cell body, its cross-sectional area passes through a maximum without an apparent shift in its centre; and (2) the depth of the cell body is correlated, albeit weakly, with the minor axis measured in the focal plane, e.g. for thirty cells in one septum long axis = $24{\cdot}1 \pm 3{\cdot}4\ \mu m$ (mean ± S.D.), short axis = $16{\cdot}9 \pm 3{\cdot}2\ \mu m$, depth = $15{\cdot}5 \pm 3{\cdot}5\ \mu m$; r (correlation coefficient) = 0·40 ($P < 0{\cdot}05$) for comparison of short axis and depth, regression line slope = 0·44; $r = 0{\cdot}02$ for comparison of long axis and depth, regression line slope = 0·02.

To calculate surface area the axes of each ganglion cell were measured at the focal plane at which the cell's cross-sectional area was largest; these axes were equated with the major and minor axes of a prolate ellipsoid, and the surface area was determined by formula.

Counting boutons. Most synaptic boutons are *en passant* rather than terminal and represent swellings of the preganglionic axon. Swellings were scored as boutons whenever a doubling in axon width occurred over a length of twenty or fewer axons widths. Thus, a swelling to 1 μm of a 0·5 μm diameter process would be scored as a bouton provided that the axon length over which the swelling occurs is less than 10 μm.

Measurement of bouton size

An estimate of bouton size was made by measuring the cross-sectional area of boutons lying on the central portion, top or bottom, of ganglion cell bodies. The outline of boutons whose centres fell within a half hemiaxis of the centre of the cell were traced onto paper using a Zeiss camera lucida attachment. The area of bouton–ganglion cell contact was measured using an Apple II Plus computer with a Houston Instruments HIPAD digitizer. The maximum error expected in measuring appositional areas of boutons that are not precisely in the focal plane is calculated to be approximately 15%.

The distribution of boutons on the cell surface

The spatial arrangement of boutons on the ganglion cell body surface was assessed by 'slicing' ganglion cells into segments having equal surface area and by analysing statistically the distribution of bouton centres on large numbers of such segments. Camera lucida drawings were made of the outlines of at least thirty ganglion cell bodies per septum, and the centre of each bouton was indicated on the cell outlines. A computer program was fed values for the major and minor axes and was used to generate values of X along the major axis such that planes orthogonal to the long axis and passing through X subtended segments of cell having equal surface area (see Fig. 4). The number of bouton centres falling on the surface of each segment was then compiled by hand and analysed statistically.

Visualizing boutons using a monoclonal antibody

In three experiments synaptic boutons on ganglion cells were visualized by immunoperoxidase techniques using a monoclonal antibody kindly provided by L. Reichardt (University of California, San Francisco). The antibody ('serum no. 30') binds to a highly conserved determinant located on the outside surface of the synaptic vesicle membrane (Matthew, Tsavaler & Reichardt, 1981). The rationale behind use of such an antibody was to test whether the nature of the relationship between bouton number and cell size as revealed by ZIO impregnation could be confirmed by independent means. Interatrial septa were fixed for 1 hr with 4% formaldehyde in 100 mM-sodium phosphate, pH 7·2, rinsed in Ringer solution plus 0·025% saponin and 2% goat serum (RGS) and incubated for 1 hr with primary antibody in RGS. Septa were then washed for 30 min in several

changes of RGS, incubated for 1 hr in biotinylated horse anti-mouse IgG (in RGS), washed for 30 min in RGS and incubated for 1 hr in avidin-biotinylated horseradish peroxidase (ABC) complex (in RGS; Hsu, Raine & Fanger, 1981; reagents obtained from Vector Labs, Burlingame, CA). Septa were then rinsed in Ringer solution, fixed in 1% glutaraldehyde in 61 mM-sodium phosphate, pH 7·2, rinsed in Ringer solution, rinsed in 0·05 M-tris (hydroxymethyl) aminomethane, pH 7·6 (Tris), and incubated first for 0·5–1·0 hr in diaminobenzidine (DAB, 0·36 mg/ml) in Tris and subsequently for 0·5–1·0 hr in DAB plus 0·05% H_2O_2 in Tris. The preparation was then rinsed in Tris, rinsed in Ringer solution, fixed for 20 min in 1% OsO_4 in 135 mM-sodium phosphate, pH 7·2 (to intensify the reaction product), rinsed in Ringer solution, dehydrated in ethanol, cleared in xylene and mounted.

Statistical procedures

Regression analysis. The best fit to the scatter diagrams was calculated by the least-squares method. The standard error of β_1 (slope) and of β_0 (y-intercept) were calculated as described by Weisberg (1980).

The Poisson distribution. The Poisson distribution was compared to both the frequency distribution of boutons per cell and the frequency distribution of boutons per 200 μm^2 cell segment. An analysis of the frequency distribution of boutons per whole cell can indicate whether the observed relationship between bouton number and cell size is explained by interaction between boutons or, alternatively, whether boutons are 'assigned' to cells independently, that is, without regard to how many other boutons are present. The scheme that permits the Poisson distribution to be compared to the observed distribution as a test of independence is as follows. The surface of each cell is divided 'on paper' into enough patches so that no more than one bouton may fall on a patch. When the patch size is sufficiently small to satisfy this criterion, the binomial distribution is in effect since there are only two outcomes per trial (zero or one bouton). Two additional consequences of making the patches small are that (1) the probability that a patch will be assigned a bouton will be also small, and (2) there will be a large number of patches per cell; thus the Poisson approximation to the binomial distribution applies. If boutons do not interact, then the probability of a success (a bouton on a patch) should be constant for all patches on a cell, and the frequency distribution of successes per n patches should be described by the Poisson theorem. The execution of the test requires a large number (N) of cells each having n patches, i.e. having an identical surface area; unfortunately, such a cell population is not available. However, since there is a direct relationship between bouton number and surface area (see Results), it is permissable to 'correct' for size by dividing by surface area; this yields a population of measurements of *bouton density* (or, alternatively, of boutons per standardized cell) whose distribution can be analysed by comparing it to the Poisson distribution. If the observed distribution is well-fitted by the Poisson distribution, then there is no need to invoke interaction between boutons in order to explain the observed relation between bouton number and cell size. If the observed distribution is significantly narrower than the Poisson distribution, then boutons are not 'assigned' to cells independently, and interaction must be invoked in order to explain why larger cells have more boutons. However, an analysis of the frequency distribution of boutons per whole cell *cannot* reveal the nature of the *spatial* distribution of boutons on the surface of individual cells. Thus, while it might be possible to say that bouton interaction does not need to be invoked to explain the correlation between bouton number and cell size, it would be quite inappropriate to conclude that the boutons are therefore randomly situated on the cell surface. In this sense the scheme mentioned above is potentially misleading, inasmuch as it discusses the notion of small membrane patches each having constant probability of being 'assigned' a bouton. One reason why an analysis based on such a scheme does not necessarily reflect the actual spatial arrangement of boutons on the cell surface is that the position of boutons on a cell may shift subsequent to the time that their number is 'determined'.

The *spatial* distribution of boutons on the cell surface *can* be determined by comparing the Poisson distribution to the frequency distribution per cell *segment*. If all patches have an equal probability of being assigned a bouton, then the frequency distribution of boutons per 200 μm^2 segment should be described by the Poisson distribution. If the observed frequency distribution is significantly narrower than the Poisson distribution, then boutons interact negatively, i.e. they tend to be evenly spaced over the surface. If the observed frequency distribution is significantly wider than the Poisson distribution, then boutons interact positively, i.e. they tend to be clustered.

Once an observed frequency distribution was obtained, the Poisson distribution was calculated

from the mean number of boutons per standardized cell (or per 200 μm^2 cell segment) and the Poisson equation. The χ^2 goodness-of-fit test was then used to compare the observed and expected distributions (Feller, 1968); the goodness-of-fit test was applied to data with $N-2$ degrees of freedom, where N is the number of bins. Data were pooled such that each bin had at least five expected observations, so that errors should be distributed normally about zero (Pearson & Hartley, 1970).

Variance ratio test. One problem associated with using the χ^2 goodness-of-fit test to analyse whether the data are described by the Poisson distribution is that a substantial loss of power occurs as a result of lumping of extreme data points (such that each bin has at least five expected observations). Lumping may obscure subtle differences between observed and expected distributions, since it is in the extreme values that these differences often are most pronounced (Simpson, Roe & Lewontin, 1960). An alternative test of the applicability of data to the Poisson distribution is the variance ratio test, which is based on the fact that the mean is equal to the variance for a Poisson distribution. In the present study this test is applied as described by Simpson *et al.* (1960).

RESULTS

The Xenopus cardiac ganglion

The organization of the cardiac ganglion in the heart of *Xenopus laevis* resembles generally that found in *Rana pipiens* (McMahan & Kuffler, 1971). Each *Xenopus* heart contains several hundred parasympathetic ganglion cells, which are innervated by preganglionic axons that project to the heart within the paired vagosympathetic nerves. The ganglion cells are found in clusters along intracardiac extensions of these nerves, which enter the heart via the sinus venosus and course toward the ventricle within both the interatrial septum and the atrial wall. The following analysis concerns only the ganglion cells lying within the interatrial septum.

Visualization of preganglionic axons

The impregnation of preterminal axons by the ZIO staining procedure (Pl. 1) permits one to map the course of the preganglionic axon as it supplies boutons to both the axon and soma of the ganglion cell. Owing to the staining of numerous preganglionic fibres within the nerve trunks in the septum, it is possible to trace axons only after they have departed from the trunk to supply individual cells; the complete pattern of innervation is therefore apparent only for neurones whose cell bodies are separate from the nerve trunk. Such cells are innervated by preganglionic axons which supply the cell body invariably by way of the proximal segment of its axon. Swellings of the preganglionic axon, representing *en passant* synapses (McMahan & Kuffler, 1971), are found on both the axon and the soma of the ganglion cell. Ganglion cell axons which are visible for some distance prior to their entering the nerve trunk may have several boutons. An analysis of forty ganglion cells having at least 20 μm of visible axon indicated that the average density of innervation is 1·2 boutons per 20 μm of axon length (ten cells examined in each of four interatrial septa).

Many ganglion cell bodies appear to be innervated by more than one stained preganglionic axon. In some instances in which the ganglion cell was separated by some distance from its nerve trunk, each of a pair of axons supplying the cell body could be seen to branch from a parent axon (see Pl. 1). It is probable that many of the ganglion cell bodies which appear to be innervated by two preganglionic axons are in fact innervated by a single axon which branches within the nerve trunk. A consequence of preganglionic axonal branching is that the number of preganglionic

motor neurones supplying a ganglion cell's soma cannot be determined by counting axons on the proximal part of its own axon. In the following analysis the number of boutons on the ganglion cell body will be analysed in relation to cell body size without regard to how many preganglionic neurones in fact give rise to those boutons.

The relation between bouton number and ganglion cell size

Casual observation of neurones stained with ZIO reveals that larger cells generally have more synaptic boutons on their surface. This correlation was quantified in eleven ZIO-stained septa. Typical results are illustrated in a scatter diagram for data pooled from two septa (Fig. 1*A*); the number of boutons is apparently directly correlated with the surface area of the cell body. Before one can conclude that this correlation is statistically significant, it is essential to demonstrate that the relationship is adequately described by a straight line. The graph of averages for the data (Fig. 1*B*) indicates that the relationship *is* approximately linear: there is no obvious tendency for the averaged values to stray from the regression line (bin size = 10 cells). A more critical analysis of linearity of the data was made by examining the residual plot (Fig. 1*C*); again there is no obvious tendency for the residuals to lie above or below the line for any cell size. A search for subtle deviations from ideal behaviour, made on the residual plot using a one-sample runs test (Siegel, 1956), shows that the data are indeed adequately described by a straight line (Fig. 1*C*, legend). The regression line for the data has the form

$$y = \beta_1 x + \beta_0,$$

where y = number of boutons, x = cell body surface area (in μm^2), β_1 = bouton density (in boutons per μm^2), and β_0 = y-intercept. The y-intercept for the data shown is $-1{\cdot}1 \pm 1{\cdot}4$ boutons (estimate $\pm$ S.E. of mean) and is not significantly different from zero (95 % confidence limits: $\pm 2{\cdot}77$ boutons). Thus the number of boutons on the cell body is directly proportional to its surface area; the relationship has a slope of $8{\cdot}4 \pm 0{\cdot}9$ boutons per 1000 μm^2 (estimate $\pm$ S.E. of mean), corresponding to one bouton per 120 μm^2 of cell body surface. The density of boutons on the cell surface is independent of ganglion cell size.

The data displayed in Fig. 1 were taken from two septa of eleven examined (animals No. 1 and 7, Table 1). Similar results were obtained on all or virtually all eleven data sets considered individually (Table 1; note the similarity of β_1 and of β_0 for the two data sets pooled to generate Fig. 1). The one-sample runs test on the residual plots demonstrated linearity in ten of eleven data sets, and all eleven estimates of β_0 were indistinguishable from zero. The over-all mean bouton density for eleven data sets was 7·9 boutons per 1000 μm^2, corresponding to one bouton per 127 μm^2 of surface area.

An expected consequence of the direct proportionality between bouton number and cell body surface is that the total area of synaptic contact, measured by summing the areas of contact of all boutons, should be proportionately larger on larger cells. This will be true provided that the *size* of individual boutons does not vary with ganglion cell size. A test of this provision was made by comparing the average bouton size on small and on large ganglion cells (bouton size measured as area of apposition, see Methods). The distribution of bouton sizes was comparable for small and for large

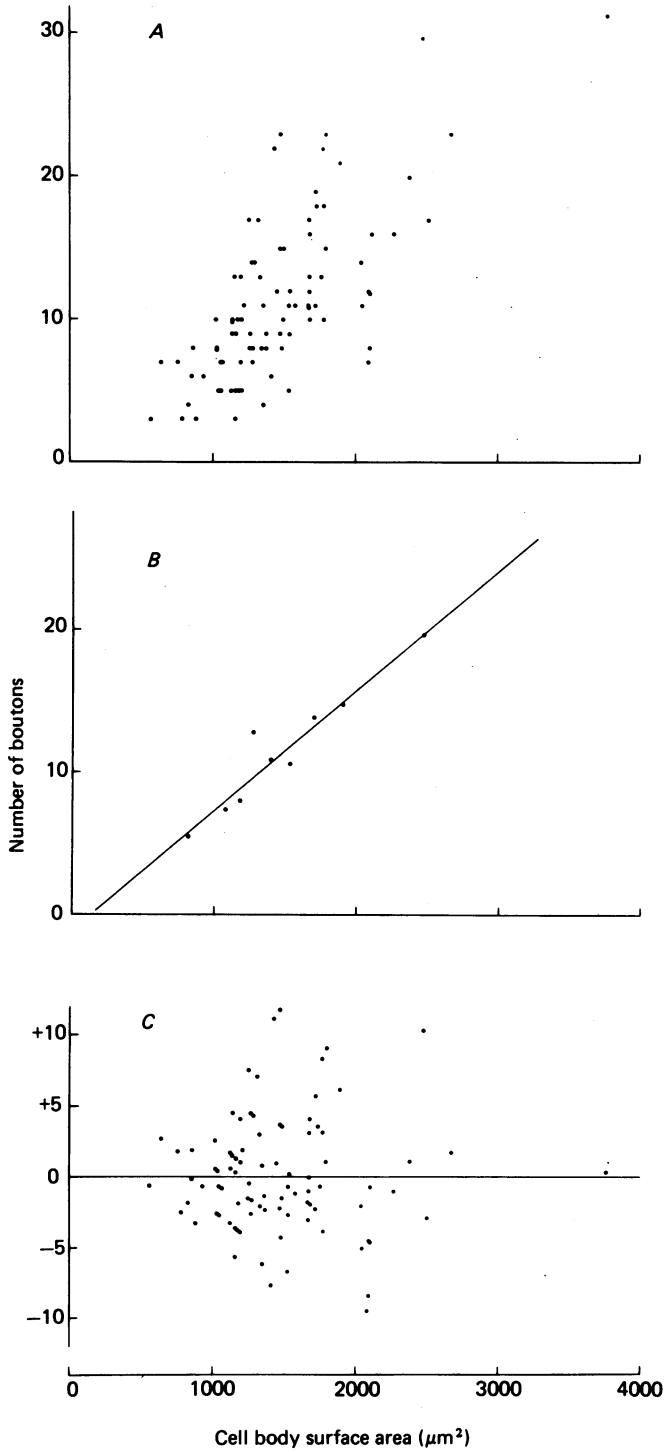

Fig. 1. For legend see opposite page.

cells (Fig. 2; the mean values were $2{\cdot}8 \pm 2{\cdot}0\ \mu m^2$ (mean $\pm$ S.D., $n = 75$) and $2{\cdot}7 \pm 1{\cdot}6\ \mu m^2$ ($n = 66$) respectively). Thus average bouton size is not dependent upon ganglion cell body size; larger cell bodies have more boutons and receive a proportionately larger area of synaptic contact than do smaller cells. The mean fraction of the cell body surface that is covered by boutons is about 2% ($2{\cdot}75\ \mu m^2$/bouton $\times$ 1 bouton/$127\ \mu m^2$), regardless of cell size. The value of 2% is similar to that (3%) calculated by McMahan & Kuffler (1971) for the fraction of the surface of cardiac ganglion cells in *Rana pipiens* covered by synaptic boutons.

The correlation between bouton number and cell size is described by a Poisson distribution

Larger cells may have more boutons because of negative interaction between boutons on the cell surface; in the extreme case boutons would assume the points of a two-dimensional lattice. If boutons displayed such territoriality, then cells having more surface area would naturally have more boutons. Alternatively, boutons may be 'assigned' to each cell in proportion to its surface area but at random, i.e. without regard to how many other boutons are assigned to that same cell. Two tests have been applied to the data to learn whether the correlation between bouton number and cell body surface is explained by negative interaction between boutons or whether it is the result of a stochastic process in which larger cells have more boutons simply because they have more places to which boutons may be 'assigned'. The results of the first test demonstrate that bouton interaction is not responsible for the observed correlation; the results of the second test (following section) demonstrate that boutons are *clustered* on the ganglion cell surface.

An examination of the pooled data of Fig. 1*A* reveals that the scatter diagram is heteroscedastic, that is, the variance tends to increase with surface area. This heteroscedasticity is characteristic of Poisson distributions, in which the variance equals the mean (Simpson *et al.* 1960). One simple test for whether the observed data are adequately described by the Poisson theorem is to examine the observed frequency distribution of boutons per standardized cell with the distribution calculated

---

Fig. 1. Direct correlation between the number of synaptic boutons on cardiac ganglion cell bodies and their surface area. *A*: a total of eighty-nine measurements from two interatrial septa (Nos. 1 and 7 of Table 1) are represented in a scatter diagram. The correlation between bouton number and cell body surface area is highly significant ($r = 0{\cdot}71$, $P < 0{\cdot}001$). The relation appears to be direct, i.e. it appears to be linear and to pass through the origin. *B*: a graph of averages of the same data as displayed in *A*. The eighty-nine measurements were ordered by surface area into bins of ten (nine in bin having largest surface area), and the average number of boutons per cell and the average cell body surface area for each bin are displayed. The line represents the regression line for the eighty-nine data points. The graph of averages reveals no obvious tendency for the data to be curvilinear. *C*: residual plot of the eighty-nine data points. Each cell is represented by a point whose x value is its size and whose y value is the difference between the actual number of boutons on its cell body and the number predicted from the regression line. The residuals tend to be distributed randomly above and below the horizontal line; this was confirmed by analysing the data using a one-sample runs test (Siegel, 1956) in which the sequence of pluses (positive residuals) and minuses (negative residuals) are ordered by surface area. The number of runs in the sequence of eighty-nine signs (plus or minus) was forty, which is well within the expected range assuming that the signs were drawn at random (probability of fewer runs = 0·17).

TABLE 1. Regression analysis of the relation between the number of boutons on the cell body and its surface area

Animal no.	No. of cells examined	Mean no. of boutons	Mean cell body surface area (μm^2)	Regression line: Slope, β_1 (boutons/$\mu m^2 \times 1000$)	Regression line: y-intercept, β_0 (boutons)	Correlation coefficient, r	One-sample runs test, P
				Zinc iodide–osmium			
1	50	11·8	1560	8·3 ± 1·1	−1·1 ± 1·7	0·76	> 0·05
2	50	10·6	1250	8·8 ± 0·9	−0·4 ± 1·3	0·80	0·03
3	50	10·4	1300	7·8 ± 1·1	0·2 ± 1·6	0·71	> 0·05
4	50	11·5	1490	7·3 ± 0·7	0·7 ± 1·2	0·83	> 0·05
5	37	8·00	1140	6·7 ± 1·4	0·3 ± 1·7	0·63	> 0·05
6	35	10·8	1780	6·2 ± 1·1	−0·3 ± 2·0	0·72	> 0·05
7	39	10·7	1360	8·6 ± 2·4	−1·1 ± 3·3	0·52	> 0·05
8	69	9·09	1460	7·9 ± 0·9	−2·4 ± 1·4	0·72	> 0·05
9	70	10·1	1480	7·0 ± 0·6	−0·3 ± 1·0	0·79	> 0·05
10	30	13·3	1370	8·3 ± 2·9	1·8 ± 4·1	0·48	> 0·05
11	30	9·73	1230	9·9 ± 2·0	−2·5 ± 2·6	0·68	> 0·05
				Immunoperoxidase			
12	50	7·42	840	9·3 ± 1·2	−0·5 ± 1·1	0·74	> 0·05
13	32	10·5	1310	6·7 ± 1·5	1·7 ± 2·1	0·61	> 0·05
14	35	15·9	1880	6·6 ± 0·8	3·4 ± 1·6	0·83	> 0·05

Regression analysis of eleven interatrial septa analysed by zinc iodide–osmium and three interatrial septa analysed by immunoperoxidase techniques are shown. Regression line slopes and y-intercepts are given as estimate ± S.E. of mean, and slopes are given as boutons per 1000 μm^2 of surface. All values of β_0 are indistinguishable from 0 ($P > 0·05$) expect No. 14 ($P = 0·05$). All values of r (correlation coefficient) indicate a significant correlation at $P < 0·001$ except No. 10 (significant at $P < 0·01$). The values of P from the one-sample runs test indicate the probability of seeing *fewer* runs of positive or negative residuals than are observed assuming they are drawn at random from a population having the same frequency of pluses and minuses as are present in the sample. None of the fourteen samples had *more* runs than expected.

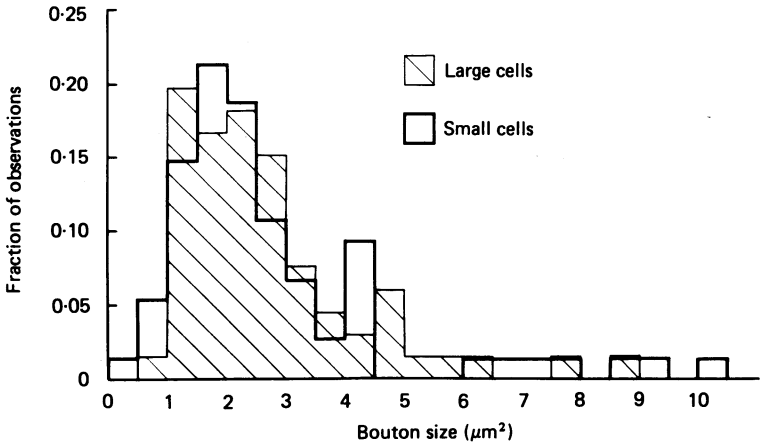

Fig. 2. Comparison between the size of synaptic boutons on large and on small cardiac ganglion cells. Bouton size was measured as the area of apposition between bouton and ganglion cell surface (see Methods). Measurements were made from two septa (Nos. 1 and 2, Table 1). Large cells analysed had long axes of 27–45 μm (lined histogram, $n = 66$ boutons); small cells analysed had long axes of 15–23 μm ($n = 75$ boutons). The two distributions are similar, and the average bouton size is therefore independent of ganglion cell size.

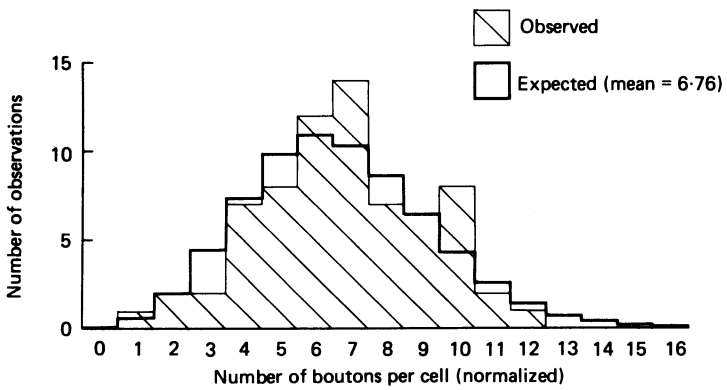

Fig. 3. Correlation between the frequency distribution of boutons per standardized cell and the Poisson distribution. The two frequency histograms represent the observed (lined) and expected distributions of boutons per standardized 1000 μm² cell body for seventy cells from a single interatrial septum (No. 9, Table 2). The expected distribution was calculated from the mean number of boutons per standardized cell (6·76, Table 2) and the Poisson equation. The two distributions have a similar shape. By the χ^2 goodness-of-fit test the probability of obtaining a worse fit, having drawn an equivalent number of measurements from a population having a Poisson distribution, is 0·73. The observed distribution is thus adequately described by the Poisson distribution.

from the mean value assuming that boutons are assigned to cells independently (see Methods for rationale). Such a comparison was made on eleven data sets, each from a separate animal. A typical result is shown in Fig. 3; the observed distribution is reasonably well approximated by the Poisson distribution generated using the mean value of boutons per standardized cell ($\lambda = 6{\cdot}76$) and the Poisson equation. By the χ^2 goodness-of-fit test $P(\chi^2) = 0{\cdot}73$, that is, under ideal conditions 73 % of comparable

observations should show a worse agreement. If the observed distributions indeed conform to the Poisson distribution, then the individual values for $P(\chi^2)$ should fall usually in the range 0·05–0·95; they in fact do (Table 2). The mean for eleven determinations of $P(\chi^2)$ was close to the ideal value of 0·5 (0·56 ± 0·23, S.D.); the observed frequency histograms are therefore adequately fitted by the Poisson

TABLE 2. Comparison of the frequency distribution of boutons per standardized cell body with the Poisson distribution

Animal no.	Boutons per 1000 μm^2 cell body: Mean	Boutons per 1000 μm^2 cell body: Variance	$P(\chi^2)$ by goodness-of-fit test	$P(\chi^2)$ by variance ratio test
		Zinc iodide–osmium		
1	7·44	7·67	0·60	0·38
2	8·17	7·90	0·63	0·50
3	7·93	8·12	0·72	0·39
4	7·89	6·97	0·18	0·33
5	7·02	4·37	0·95	0·05
6	6·02	5·86	0·49	0·55
7	7·86	9·00	0·36	0·21
8	6·09	5·90	0·64	0·48
9	6·67	4·84	0·73	0·05
10	9·44	13·40	0·25	0·05
11	7·78	8·12	0·65	0·35
		Immunoperoxidase		
12	8·74	8·35	0·82	0·48
13	8·58	2·56	< 0·001	< 0·001
14	8·14	9·67	0·49	0·18

The mean values for boutons per 1000 μm^2 cell body are determined from individual, standardized values. The number of cells used to calculate each value can be found in Table 1. $P(\chi^2)$ by the χ^2 goodness-of-fit test gives the probability of seeing a worse fit than that observed assuming that the samples were drawn at random from a population having the indicated mean and a Poisson distribution (see Fig. 3 for an example of one comparison). Ideally the P value should fall usually in the range 0·05–0·95. $P(\chi^2)$ by the variance ratio test denotes the probability that the sample was drawn from a population having a Poisson distribution (calculated according to Simpson *et al.* 1960). By both criteria only one data set (No. 13) is clearly non-Poisson.

distribution as determined using the goodness-of-fit test. The data were also analysed by the variance ratio test, which is more sensitive than the goodness-of-fit test (see Methods). The variance ratio test relies on the fact that the mean and variance of a Poisson distribution are equal. Using this test eight of the eleven data sets are adequately described by the Poisson theorem ($P > 0·05$, Table 2). The remaining three data sets had probabilities of 0·05, indicating a marginally significant fit. Thus, by a stringent test a majority of the data sets are Poisson, and none of them are distributed in a significantly non-Poisson manner. This validates the assumption that boutons are 'assigned' to cells independently. There is no need to invoke bouton interaction of any kind in order to explain the observed correlation between bouton number and cell size. This correlation is the result of a stochastic process: larger cells have more boutons because they have more membrane patches to which boutons might be 'assigned'.

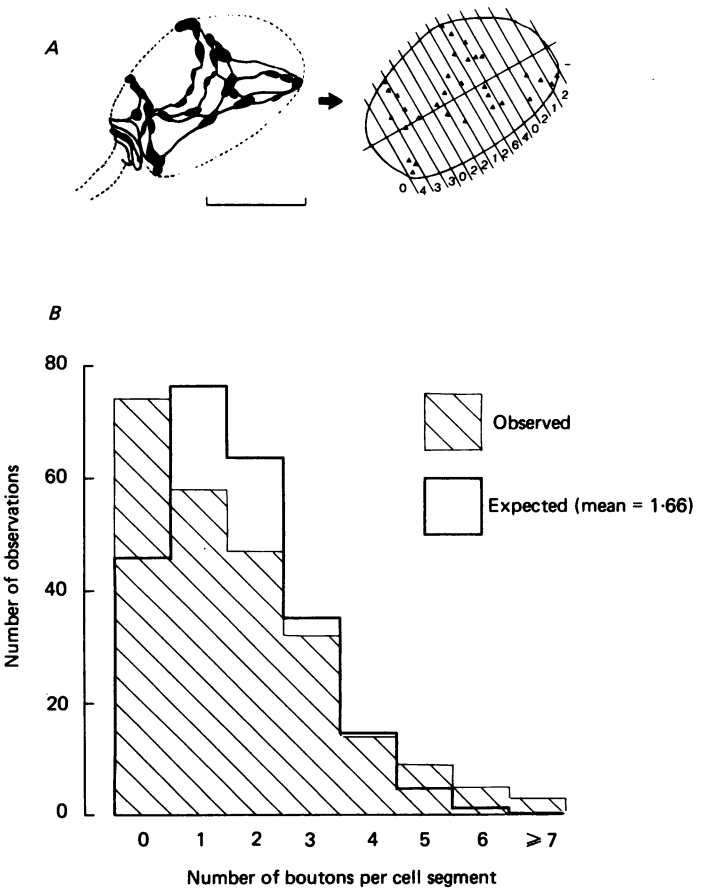

Fig. 4. Comparison between the frequency distribution of boutons-per-cell-body-segment and the Poisson distribution. The spatial distribution of boutons on the cell surface was analysed by noting the number of boutons falling on cell body segments having a 200 μm^2 surface area, as indicated schematically in *A*. With the aid of a light microscope and a camera lucida attachment, the centre of each bouton (*A*, left; bar, 20 μm) is superimposed upon an outline of the cell body (*A*, right, triangles). The major axis of the cell is drawn, and a computer program is utilized to generate points along the major axis, starting at the base of the cell, such that planes orthogonal to the axis and drawn through the points subtend equal increments of cell surface area (200 μm^2). (The cell bodies are assumed to be prolate ellipsoids.) The number of centres falling in each 200 μm^2 segment is noted (*A*, right). Partial segments are not included in the analysis. The observed distribution (*B*, lined histogram) was taken from an analysis of 242 segments from thirty-nine cells in one interatrial septum (No. 7, Table 2). The expected distribution was calculated from the mean number of bouton centres per segment ($\lambda = 1{\cdot}66$). The observed distribution is not well fitted by the Poisson distribution; there are too many observations at extreme values of boutons-per-segment and too few observations at values near the mean. By the χ^2 goodness-of-fit test the probability of obtaining a worse fit, having drawn an equivalent number of measurements from a population having a Poisson distribution, is 0·000001. Thus the observed distribution is non-Poisson; the deviation between observed and expected distributions is explained by clustering of boutons on the cell surface.

The spatial distribution of boutons on the ganglion cell surface

While the analysis of the observed *frequency* distribution of boutons per cell indicates that bouton interaction is not responsible for generating the observed relationship between bouton number and cell size, this analysis does not reveal how boutons are actually distributed on the cell surface. The *spatial* distribution of boutons can be discerned by analysing the frequency distribution of boutons falling on cell segments of constant surface area. A number of cells (thirty to forty) in each of five septa were divided into segments having a surface area of 200 μm^2 to produce five samples of cell segments (Fig. 4*A* demonstrates schematically how this is done).

TABLE 3. Comparison of the distribution of boutons per 200 μm^2 cell body segment with the Poisson distribution

Animal no.	No. of cell segments examined	Boutons per segment (mean)	$P(\chi^2)$
	Zinc iodide–osmium		
5	189	1·48	0·002
6	285	1·29	< 0·001
7	242	1·66	< 0·001
10	192	1·93	0·025
11	171	1·56	0·830
	Immunoperoxidase		
13	284	1·75	0·015
14	210	1·64	0·007

$P(\chi^2)$ by the χ^2 goodness-of-fit test denotes the probability of seeing a worse fit than that observed assuming that the samples were drawn at random from a population having the indicated mean and a Poisson distribution (see Fig. 4*B* for an example of one comparison). Six of the seven data sets show a poor fit; in all six the distribution was significantly broader than that expected (as in Fig. 4*B*). In one data set (No. 11), the observed distribution is well fit by the Poisson distribution. In no instance was the distribution narrower than a Poisson distribution, as would be expected if there were negative interaction among boutons.

For each sample the distribution of boutons-per-segment was compared to that expected from a Poisson distribution. The analysis from one animal is shown in Fig. 4*B*; the observed distribution has a markedly different shape from the Poisson distribution; there are more segments having no boutons and more segments having five or more boutons than predicted, and there are fewer segments having one, two or three boutons than predicted. The observed distribution is not well fitted by the Poisson distribution; the probability that such a discrepancy would occur by chance is 0·000001 (χ^2 goodness-of-fit test). Thus the boutons on cells in this sample are not randomly distributed: they interact. The interaction, however, is of the opposite sense as that needed to explain the observed correlation between bouton number and cell size; boutons tend to be clustered on the cell surface rather than evenly spaced. Four of the five data sets analysed in a like manner showed evidence of positive interaction between boutons, and one data set showed a distribution that was approximately Poisson in nature (Table 3). In general, boutons are not randomly distributed on the surface of the ganglion cell but tend to cluster. This result does not conflict with the

analysis done on whole cells, which revealed that bouton interaction does not contribute to the observed relationship between bouton number and cell size. Thus while boutons tend to cluster on the cell surface, the mechanism that results in larger cells having more boutons is not influenced by bouton–bouton interaction.

Visualizing synaptic boutons using immunoperoxidase techniques

The zinc iodide-osmium technique results in staining of both synaptic boutons and the terminal portion of the preganglionic axon; the boutons are usually *en passant* swellings of the axon. Since the decision as to what sort of swelling constitutes a bouton is made arbitrarily (see Methods), it would be useful to collect and analyse data based on an independent means of visualizing boutons. Synaptic boutons were therefore stained by immunoperoxidase techniques using a monoclonal antibody that recognizes a determinant on the synaptic vesicle membrane (Matthew *et al.* 1981). The pattern of bouton staining using this antibody resembled that seen with zinc iodide and osmium. The major differences between the two procedures were that the immunoperoxidase technique (1) did not stain organelles within the ganglion cell body, (2) did not stain the preganglionic axons, and (3) did not produce a reaction product in boutons as dense as that produced by zinc iodide and osmium. All the conclusions that can be made from ZIO staining about the correlation between bouton number and cell size and about its nature can also be made on the basis of the three septa stained with the monoclonal antibody (Tables 1–3). Thus:

(1) The number of boutons was strongly correlated with cell body surface area (Table 1); the relationship was linear with a slope corresponding to one bouton per 140 μm^2 (Table 1) and an intercept which was not significantly different from zero (in two of three instances).

(2) The frequency distribution of boutons per normalized cell was distributed roughly according to the Poisson distribution by the χ^2 goodness-of-fit test and the variance ratio test (Table 2; note, however, that data set No. 13 was *not* distributed according to the Poisson theorem; this data set was the only one of fourteen samples with a variance too small to have been drawn from a population having a Poisson distribution).

(3) The spatial distribution of boutons on the cell surface was *not* random, but rather indicative of bouton clustering (Table 3).

DISCUSSION

Before the evidence for a direct relationship between bouton number and cell body surface area can be reviewed, it is useful to consider the possible sources of error in estimation of both parameters. In scoring axonal swellings as synaptic boutons it has been assumed (1) that all synapses have been rendered visible by ZIO impregnation, and (2) that there is a one-to-one correspondence between swellings of the preganglionic axon and synaptic boutons. The first of these assumptions has been validated by electron microscopy; the zinc iodide–osmium procedure used here darkly impregnates all synapses in all preparations (see Methods). The second assumption implies that all swellings of the preganglionic axon represent synaptic boutons, and, conversely, that all synaptic boutons are represented by swellings of the preganglionic axon. The

similarity between the results obtained with the ZIO technique and with immunoperoxidase techniques using an anti-synaptic vesicle antibody (Table 1) imply that the number of axon swellings is equivalent to the number of synaptic boutons; thus the average density of boutons per unit of cell surface area is similar using as a criterion for synaptic boutons either the presence of an axonal swelling or the presence of synaptic vesicles. It is unlikely that both techniques would fortuitously underestimate the actual number of boutons by comparable amounts; rather, it is probable that both are quantitative.

Some error is likely to have occurred in estimating the surface area of ganglion cell bodies. It has been assumed that the cell bodies are shaped like prolate ellipsoids, with their major axis in the plane of the interatrial septum. This assumption is unlikely to be completely correct; first, ganglion cells often do *not* have a precise elliptical shape: the radius of curvature at their poles is often greater than that expected of a true ellipse (Pl. 2*A*), and second, the minor axis in the plane of the interatrial septum is only weakly correlated with the depth of the cell (see Methods). Ganglion cells may therefore have a very complicated shape, and their exact surface area may not be readily estimated. The estimates made here may be reasonably accurate, however, since the two known sources of systematic error (too much curvature at the poles and too little depth for the width) should tend to counteract one another. Any systematic error arising from these or other factors could profoundly influence the conclusions only if it affected the estimation of surface area on small and large cells *differentially*. In the absence of such errors, it is apparent that bouton number is directly related to surface area and that the correlation between the two parameters is highly significant. The mean bouton number is related to the mean surface area by a simple constant, bouton density. The density of innervation, expressed as boutons per square micrometre, remains constant for ganglion cell bodies whose surface areas vary over a ten-fold range. Since the *size* of boutons remains constant over this range, boutons cover on average a constant fraction (2%) of the cell body surface, regardless of cell size. A qualitatively similar relationship has been documented for other synapses. At both amphibian and mammalian neuromuscular junctions the size of the motor nerve terminal appears to be directly related to the diameter of the myofibre it suplies; (Nyström, 1968; Kuno *et al.* 1971; Korneliussen & Waerhung, 1973), and in the optic neuropile of the fly's eye the number of synapses made by receptor neurones onto dendritic branches of laminar neurones is directly related to dendritic surface area (Nicol & Meinertzhagen, 1982).

Nature of the correlation between bouton number and surface area

The statistical tests used here were designed to address the hypothesis that a negative interaction between boutons is responsible for the fact that larger cells have correspondingly more boutons. All tests applied to the data negated this hypothesis. The first pair of tests (goodness-of-fit and variance ratio test, Table 2) analysed whether the frequency distribution of bouton densities (boutons per standardized cell) was any narrower than that expected from a stochastic process; it was not. The third statistical test directly addressed the negative interaction hypothesis by examining the *spatial* distribution of boutons on the cell surface. This third test revealed that boutons tend to be clustered; thus they interact positively rather

than negatively. Thus, while boutons tend to cluster on the cell surface, their number per standardized cell is distributed in a random fashion.

It is not surprising that boutons cluster on the cell surface; they arise from axons and are likely to be found in higher density on those parts of the cell more densely supplied by preganglionic axons. The density of boutons is in fact higher on cell segments closer to the base of the cell, where the preganglionic axon tends to wrap itself around the cell body before branching to supply the distal parts of the cell. McMahan & Kuffler (1971) have noted a similar clustering of boutons at the base of cardiac ganglion cells in *Rana*. The tendency for boutons to be clustered is somewhat stronger in *Rana* than in *Xenopus*, where the probability of finding a bouton at the base of the cell is about twice as high as that of finding a bouton at its opposite pole (data not shown).

Functional implications

The correlation of bouton number, but not bouton size, with cell body surface area implies that the total area of synaptic contact on ganglion cells is regulated by varying the *number* of individual boutons and not their size.

The fact that small and large cells alike have a constant fraction (2 %) of their cell surface covered with boutons may have functional implications. If each bouton releases a constant amount of transmitter, then larger cells should have proportionately more transmitter released onto their cell bodies. The expected increase in transmitter release on larger cells should generate more synaptic current and would be expected to 'counteract' the corresponding decrease in their input resistance. In muscle such an effect is known to occur; synapses on large myofibres are larger physically and transmit with larger quantal content than synapses on small myofibres (Kuno *et al.* 1971; Harris & Ribchester, 1979; Grinnell & Herrera, 1980; see also Angaut-Petit & Mallart, 1979). The effect of the correlation between ganglion cell surface area and bouton number might therefore be to 'correct' for cell size and to assure a constant safety factor. Unfortunately, it is difficult to assess how reasonable this expectation might be; a critical assumption is that of a proportionality between the number of boutons and the amount of transmitter release. Although there is evidence that the number of boutons can be correlated with the physiologically measured release parameter, n (Korn, Mallet, Triller & Faber, 1982; see also Roper, 1976), recent work by Nudell & Grinnell (1982) shows that transmitter output can be *inversely* correlated with terminal size on muscle fibres having similar input resistance. A second potential criticism of the expectation that the correlation demonstrated here will tend to assure a constant safety factor is that it ignores the synaptic boutons on the ganglion cell's axon; these may contribute substantially to the synaptic current that brings the ganglion cell to threshold.

Why do larger ganglion cells have more boutons?

The applicability of a stochastic model in explaining the correlation between bouton number and surface area does not eliminate the need for an understanding of why larger cells have more boutons. There are three possible explanations for the observed correlation. The first is that the number of synaptic boutons may increase to 'compensate' for growth of the ganglion cell body; thus, ganglion cell growth may

be an independent event and synaptic proliferation a dependent one. Conversely, synaptic proliferation may be the independent event: differential proliferation may induce differential ganglion cell growth. Finally, both ganglion cell growth and synaptic proliferation may be dependent upon other, as yet unspecified events. A study of the growth of ganglion cells and of their innervation during larval and post-metamorphic life may afford an opportunity to distinguish among these possibilities.

I thank Doug Evans for his participation in the early stages of this project, Bill Carlson, Roger Kornberg, Larry Maloney, Mike Letinsky, Chuck Stevens and Brian Wandell for helpful suggestions, Lou Reichardt for his gift of antibody no. 30, Jack McMahan for the use of computer facilities, Denis Baylor and Carla Shatz for their critical reading of a draft of this manuscript, and Diane Hill and Jeannie Lukas for their typing. This work was supported by the National Science Foundation, by Basil O'Connor Starter Research Grant No. 5-300 from the March of Dimes Birth Defects Foundation, by the Dysautonomia Foundation and by institutionally administered grants from the National Institutes of Health (Biomedical Research Support Grant no. RR5353) and the American Cancer Society.

REFERENCES

AKERT, K. & SANDRI, C. (1968). An electron-microscopic study of zinc-osmium impregnation of neurons. I. Staining of synaptic vesicles at cholinergic junctions. *Brain Res.* **7**, 286–295.

ANGAUT-PETIT, D. & MALLART, A. (1979). Dual innervation of end plate sites and its consequences for neuromuscular transmission in muscles of adult *Xenopus laevis*. *J. Physiol.* **289**, 203–218.

BENNETT, M. R. & RAFTOS, J. (1977). The formation and regression of synapses during the re-innervation of axolotl striated muscles. *J. Physiol.* **265**, 261–295.

COËRS, C. (1955). Les variations structurelles normales et pathiologiques de la jonction neuromusculaire. *Acta neurol. psychiat. belg.* **55**, 741–866.

FELLER, W. (1968). *An Introduction to Probability Theory and Its Applications*, vol. I., pp. 156–164. New York: Wiley.

GRINNELL, A. D. & HERRERA, A. A. (1980). Physiological regulation of synaptic effectiveness at frog neuromuscular junctions. *J. Physiol.* **307**, 301–317.

HARRIS, C. (1954). The morphology of the myoneural junction as influenced by neurotoxic drugs. *Am. J. Path.* **30**, 501–519.

HARRIS, J. B. & RIBCHESTER, R. R. (1979). The relationship between end-plate size and transmitter release in normal and dystrophic muscles of the mouse. *J. Physiol.* **296**, 245–265.

HEUSER, J. E. & REESE, T. S. (1973). Evidence for recycling of synaptic vesicle membrane during transmitter release at the frog neuromuscular junction. *J. Cell Biol.* **57**, 315–344.

HSU, S. M., RAINE, L. & FANGER, H. (1981). The use of avidin–biotin–peroxidase complex (ABC) in immunoperoxidase techniques. A comparison between ABC and unlabeled antibody (PAP) procedures. *J. Histochem. Cytochem.* **29**, 577–580.

KORN, H., MALLET, A., TRILLER, A. & FABER, D. S. (1982). Transmission at a central inhibitory synapse. II. Quantal description of release with a physical correlate for binomial n. *J. Neurophysiol.* **48**, 679–707.

KORNELIUSSEN, H. & WAERHUNG, O. (1973). Three morphological types of motor nerve terminals in the rat diaphragm, and their possible innervation of different muscle fiber types. *Z. Anat. EntwGesch.* **140**, 73–84.

KUNO, M., TURKANIS, S. A. & WEAKLY, J. N. (1971). Correlation between nerve terminal size and transmitter release at the neuromuscular junction of the frog. *J. Physiol.* **213**, 545–556.

MAILLET, M. (1962). La technique de Champy a l'osmium iodure de potassium et la modification de Maillet a l'osmium-iodure de zinc. *Trab. Inst. Cajal Invest. biol.* **54**, 1–36.

MATTHEW, W. D., TSAVALER, L. & REICHARDT, L. F. (1981). Identification of a synaptic vesicle-specific membrane protein with a wide distribution in neuronal and neurosecretory tissue. *J. Cell Biol.* **91**, 257–269.

McMAHAN, U. J. & KUFFLER, S. W. (1971). Visual identification of synaptic boutons on living ganglion cells and of varicosities in postganglionic axons in the heart of the frog. *Proc. R. Soc.* B **177**, 485–508.

NICOL, D. & MEINERTZHAGEN, I. A. (1982). Regulation in the number of fly photoreceptor synapses: the effects of alterations in the number of presynaptic cells. *J. comp. Neurol.* **207**, 45–60.

NUDELL, B. M. & GRINNELL, A. D. (1982). Inverse relationship between transmitter release and terminal length in synapses on frog muscle fibers of uniform input resistance. *J. Neurosci.* **2**, 216–224.

NYSTRÖM, B. (1968). Postnatal development of motor nerve terminals in 'slow-red' and 'fast-white' cat muscles. *Acta. neurol. psychiat. scand.* **44**, 363–383.

PEARSON, E. S. & HARTLEY, H. D. (1970). *Biometrika Tables for Statisticians*, 3rd edn., vol I, pp. 10–11. Cambridge: University Press.

ROPER, S. (1976). An electrophysiological study of chemical and electrical synapses on neurones in the parasympathetic cardiac ganglion of the mudpuppy, *Necturus maculosus*: evidence for intrinsic ganglionic innervation. *J. Physiol.* **254**, 427–454.

SARGENT, P. B. (1982). The number of synaptic boutons terminating on autonomic neurons is correlated with cell size. *Soc. Neurosci. Abstr.* **8**, 279.

SARGENT, P. B. & EVANS, C. D. (1981). Quantitative staining of synapses on frog cardiac ganglion cells using zinc-iodide and osmium. *Soc. Neurosci. Abstr.* **7**, 671.

SIEGEL, S. (1956). *Nonparametric Statistics for the Behavioral Sciences*, pp. 52–58. New York: McGraw-Hill.

SIMPSON, G. G., ROE, A. & LEWONTIN, R. C. (1960). *Quantitative Zoology*, pp. 310–312. New York: Harcourt, Brace and World.

WEISBERG, S., (1980). *Applied Linear Regression*, pp. 13–14. New York: Wiley.

EXPLANATION OF PLATES

PLATE 1

Light micrographs of a *Xenopus* cardiac ganglion cell stained with zinc iodide and osmium. *A*, *B*, *C*, micrographs taken at different focal planes using differential interference contrast optics (Nomarski). *A*, micrograph taken while focusing on the middle of the cell showing a nucleus and a pair of stained preganglionic axons supplying the ganglion cell body by way of its axon. The two stained axons are branches of a single axon (see *D*). *B* and *C*, micrographs taken while focusing on the upper and lower surfaces of the cell. Several stained synaptic boutons are visible. The stained granules within the cytoplasm are lysosomes. *D*, camera lucida drawing of the complete pattern of innervation of the cell body. The cell body is supplied with fifteen synaptic boutons. The dashed lines indicate the outline of the ganglion cell and of satellite cell bodies at the base of the ganglion cell body. The dotted line indicates the edge of the nerve trunk. Both stained axons that supply the ganglion cell body arise from a swelling barely visible in *A*. Bar (in *D*), 20 μm.

PLATE 2

Electron micrographs of a *Xenopus* cardiac ganglion cell stained with zinc iodide and osmium (ZIO) under approximately iso-osmotic conditions (280 m-osM). *A*, a ganglion cell body is seen surrounded by satellite cell processes. Stained structures include synaptic boutons at the cell surface and lysosomes in the cell's interior. Reaction product is associated with the extracellular matrix (see also *B*). Bar, 5 μm. *B*, synaptic bouton impregnated with stain (same field as in *A*). This is identified as a synapse by virtue of the prominent post-synaptic density. The nerve terminal is densely stained. Impregnated synaptic vesicles (arrows) can sometimes be recognized but are often difficult to distinguish from reaction deposits. Large, dense-cored vesicles are not impregnated with stain and are often the most electron-lucent structures within the terminal (arrowhead). Bar, 0·5 μm.

PLATE 3

Electron micrographs of a *Xenopus* cardiac ganglion cell stained with zinc iodide and osmium (ZIO) under hyperosmotic conditions (550 m-osM). *A*, a ganglion cell body surrounded by satellite cell processes. The surface of the ganglion cell is crenulated, presumably due to the loss of water from the ganglion cell and its accumulation in 'pockets' beneath the satellite cell. Quantitative measurements (see Methods) show, however, that the hyperosmotic staining solution does not produce any detectable shrinkage when compared to the roughly iso-osmotic solution (Pl. 2*A*). Stained structures include synaptic boutons at the cell surface and lysosomes in the cell's interior. Bar, 5 μm. *B*, a pair of stained nerve terminals (different field from *A*). Only the terminal on the left has a clear post-synaptic density and would have been scored as a bouton for the purposes of evaluating the usefulness of the ZIO procedure as a quantitative stain for synapses. The density of nerve terminal stain is similar to that in Pl. 2*B*; in general, terminals are *more* densely stained with reaction product when treated with the hyperosmotic ZIO formulation. Bar, 1 μm.

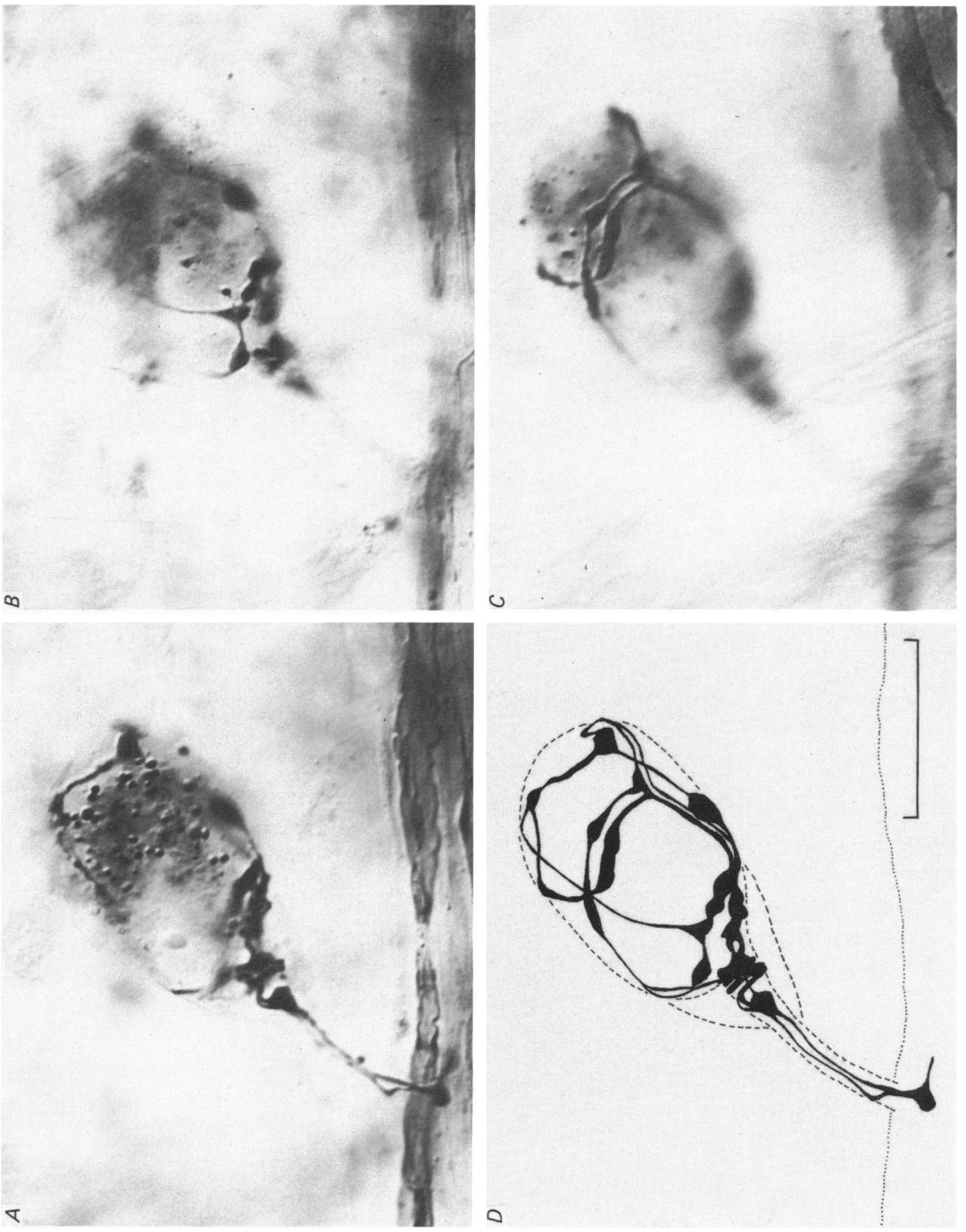

(*Facing p.* 104)

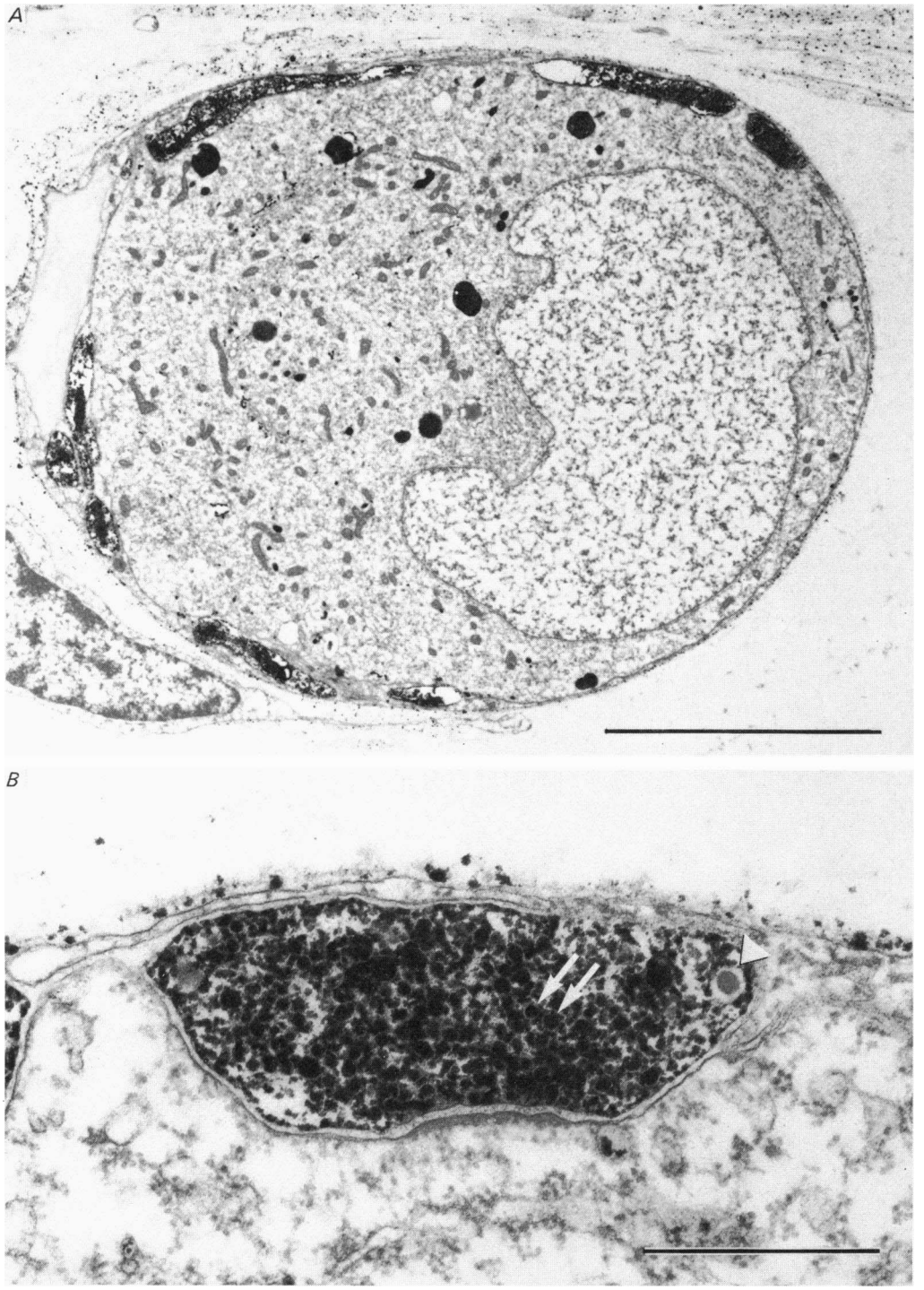
A
B

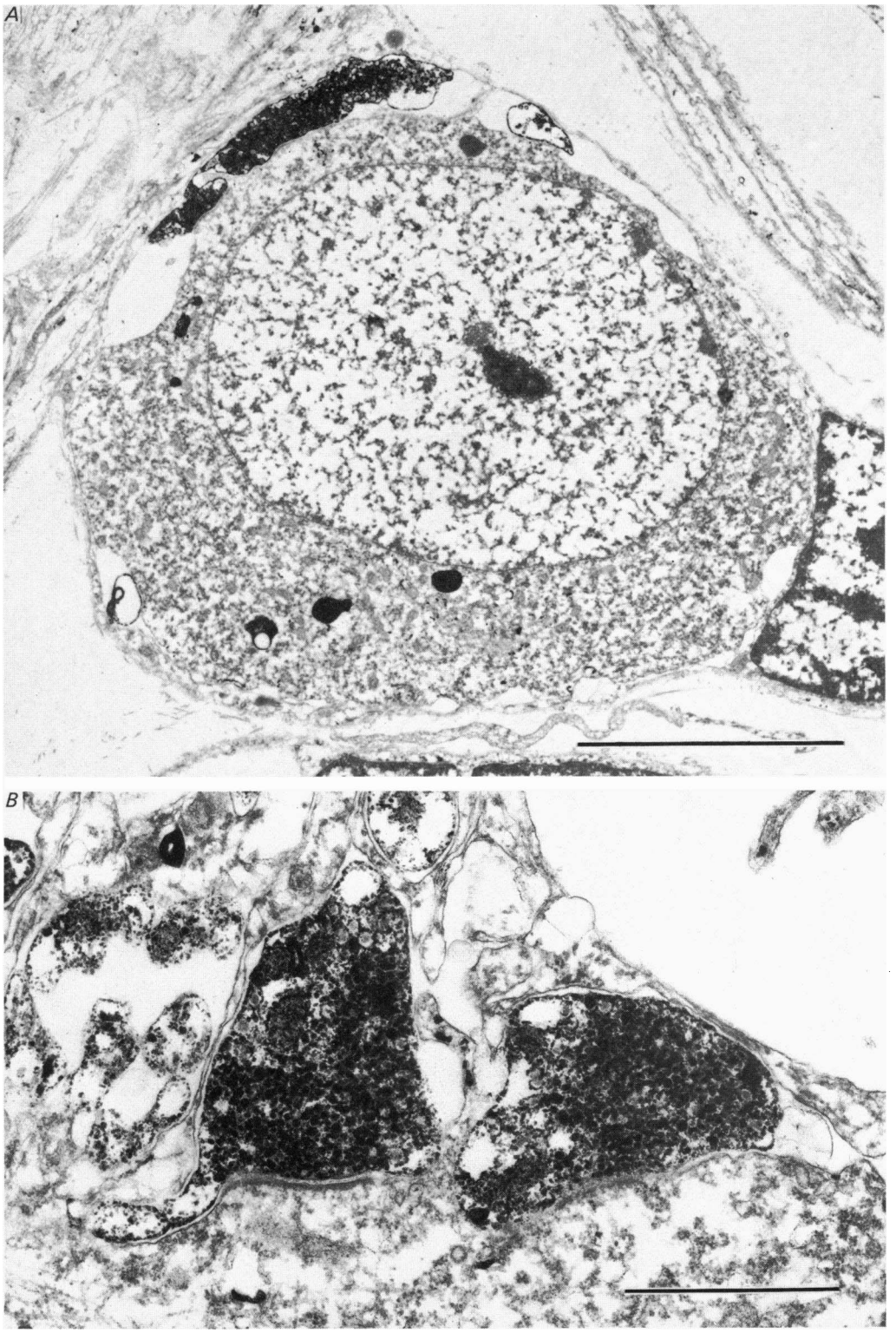
A
B